Diffusible Cross-linkers Cause Superexponential Friction Forces

Harmen Wierenga and Pieter Rein ten Wolde*
AMOLF, Science Park 104, 1098 XG Amsterdam, Netherlands

(Received 19 September 2019; accepted 15 July 2020; published 12 August 2020)

The friction between cytoskeletal filaments is of central importance for the formation of cellular structures such as the mitotic spindle and the cytokinetic ring. This friction is caused by passive cross-linkers, yet the underlying mechanism and the dependence on cross-linker density are poorly understood. Here, we use theory and computer simulations to study the friction between two filaments that are cross-linked by passive proteins, which can hop between discrete binding sites while physically excluding each other. The simulations reveal that filaments move via rare discrete jumps, which are associated with free-energy barrier crossings. We identify the reaction coordinate that governs the relative microtubule movement and derive an exact analytical expression for the free-energy barrier and the friction coefficient. Our analysis not only elucidates the molecular mechanism underlying cross-linker-induced filament friction, but also predicts that the friction coefficient scales superexponentially with the density of cross-linkers.

DOI: 10.1103/PhysRevLett.125.078101

The formation of cytoskeletal structures like the mitotic spindle [1–15] and the cytokinetic ring [16–19] depends not only on motor proteins, but also on nonmotor proteins that cross-link the filaments passively. Force generation is often attributed to the motor proteins, but passive cross-linkers can generate driving forces too, via their condensation to the overlap between the filaments [19,20] or via the entropy associated with their diffusion within the overlap region [21]. Yet, in these highly dynamic systems both active and passive cross-linkers also create frictional forces, which oppose the motor, condensation, or entropic driving forces. These frictional forces are a central determinant of the mechanical properties of cytoskeletal structures [22], limit the speed and efficiency with which these structures are formed [19,23–25], and can even be vital for their stability because motor forces need to be balanced by stabilizing passive cross-linkers [3,6–10]. Furthermore, asymmetric friction forces can harness active filament fluctuations to generate directed motion of passive cross-linkers [26] and enhance the motion of motor proteins [27].

Friction in cellular systems has been studied theoretically. Prandtl-Tomlinson models [28], in which a particle moves over a sinusoidal potential, have been used to study how protein-filament [26,29,30] and filament-filament [22] friction depends on the velocity [22,26,29,30] and the polarity of the filaments [22,26,29]. The Frenkel-Kontorova model [28], in which filaments consist of units connected via springs, has been employed to study how the contact friction depends on the overlap length between filaments [22]. Huxley-Lacker-Peskin type models, in which rigid filaments interact through cross-linkers that are modeled as harmonic springs that bind to a continuum or discrete set of binding sites [31–36] have been used to investigate force-velocity relations, and how these depend on the stiffness of the cross-linkers and the underlying substrate, and on the rates of cross-linker-filament attachment and detachment [20,36,37].

Yet, to understand the size of cytoskeletal structures such as the mitotic spindle and the cytokinetic ring, the speed and efficiency with they are formed, and the forces they can generate, it is vital to understand how the friction coefficient depends on the number of cross-linkers and on the overlap length between filaments [38]. Previous models either assume [7,26,39–41] or would predict [20,37,42] that the friction scales linearly with the number of cross-linkers.

Recent *in vitro* experiments have demonstrated that a protein from the Ase1/PRC1 family, which passively cross-links microtubules in the mitotic spindle, generates friction forces that do not scale linearly but rather exponentially with the number of cross-linkers in the overlap region [21]. The system exhibits generic features that are also found in other systems, such as the cytokinetic ring [19]. In particular, the filaments consist of a regular lattice of subunits that are of similar size as the cross-linkers. The cross-linkers thus bind to a discrete set of binding sites, while they are also stiff on the length scale set by the spacing between the binding sites, as discussed in more detail below. These assumptions are in marked contrast to the continuum of binding sites in the current theoretical models that predict a linear scaling of the friction with the number of cross-linkers [20,37,42].

Here, we present a model in which cross-linkers hop between discrete binding sites in the overlap region (Fig. 1). Our analysis shows that the discrete nature of the binding sites combined with the stiffness of the cross-linkers makes that the filaments can only move if the cross-linkers reorganize collectively. This turns filament movement into an activated process with an energy barrier that scales

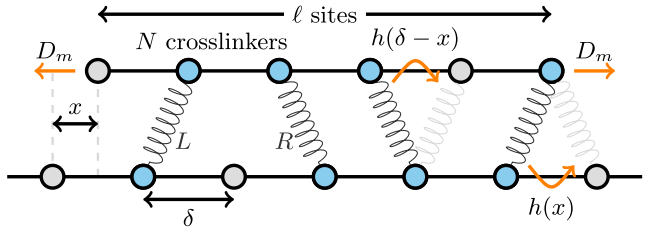

FIG. 1. Model of the microtubule overlap. The filaments are represented as one-dimensional lattices with spacing δ and are connected by cross-linking proteins, described as springs. The bottom filament is fixed, while the top filament can move in the longitudinal direction due to Brownian motion with diffusion constant D_m or the pulling of stretched cross-linkers. Cross-linkers can make a diffusive step, causing them to switch from right-pulling linkers labeled R to left-pulling linkers denoted L, or vice versa. Two of such possible transitions, together with their rates h, are indicated by orange arrows. The fixed microtubule is infinitely long and the mobile one has ℓ lattice sites. There are N cross-linkers connecting the two filaments, which stay bound indefinitely.

linearly with the number of cross-linkers. It explains why the friction scales exponentially with the number of cross-linkers. At higher densities our model predicts that the friction scales superexponentially with the number of cross-linkers, because of an entropic effect caused by steric hindrance.

Our model is shown in Fig. 1. It resembles the experimental setup used to measure the filament friction generated by Ase1 cross-linkers *in vitro* [21]. We probe the friction though a small mobile microtubule connected via cross-linkers to a microtubule that is fixed on the bottom. The top microtubule shows one-dimensional movement parallel to the bottom one, and we avoid entropic force generation by having a constant overlap length [21]. Both microtubules contain a one-dimensional lattice of binding sites with spacing $\delta = 8$ nm [43,44], and cross-linkers can hop between neighboring sites while they physically exclude each other.

To allow for movement of both the microtubule and the linkers, cross-linkers can stretch as Hookean springs with spring constant k and both ends of each linker can hop to empty neighboring binding sites. The effective parameter k is estimated from experimental data by observing how the diffusion constant of cross-linkers in overlaps is reduced compared to that of proteins on a single microtubule (Sec. S.I of the Supplemental Material [45]). We find $k = 1.1 \times 10^5\ k_B T/\mu\text{m}^2$, which is comparable to values reported for similar proteins [35,46–48]. This value strongly suppresses stretching more than δ, and to facilitate model analysis and speed up simulations, we choose to impose a maximum stretch of one lattice spacing.

The position of the mobile microtubule relative to the fixed one is called x, such that x modulo δ represents the misalignment of the two lattices. The requirement that the cross-linking springs are extended less than one lattice spacing only allows for springs that are extended horizontally by a distance of either x or $\delta - x$. These are respectively called left- and right-pulling cross-linkers (Fig. 1). We model the movement of the top microtubule using Brownian dynamics with an intrinsic drag coefficient [49], and implement cross-linker hops through a kinetic Monte Carlo algorithm [50] (Sec. S.II of the Supplemental Material [45]).

Ase1/PRC1 (un)binding from the microtubule overlap plays no role in the *in vitro* friction experiments [21], leading us to exclude these reactions. Ignoring binding effects reduces the number of parameters, and allows us to focus on the specific dependence of the friction on the absolute number of cross-linkers in the microtubule overlap region N, and on the size of this region—the number of lattice sites on the mobile microtubule ℓ.

We visualize the dynamics of the mobile microtubule using computer simulations in Fig. 2. The position of the top filament makes discrete jumps between points $\{x : x \equiv 0 (\text{mod}\, \delta)\}$, where cross-linkers are energetically relaxed. The waiting time between jumps is exponentially distributed with rate $2r$ (Sec. S.III of the Supplemental Material [45]), which suggests that a single barrier exists between these states.

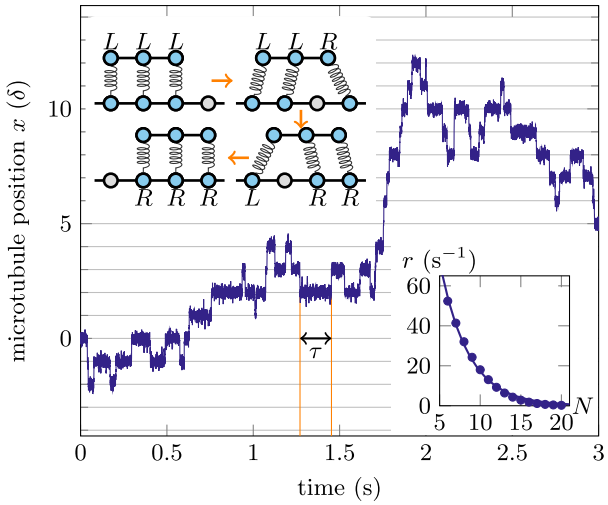

FIG. 2. A typical time trace of the mobile microtubule position shows that it moves with sudden jumps. Horizontal lines denote positions where the microtubules are in register. The jumps occur at a fixed rate in both directions, which can be estimated from the mean waiting time in simulations, $r = 1/2\bar{\tau}$. (inset, top-left) A typical transition, where the microtubules begin and end in register. Cross-linkers are stretched in intermediate states, which energetically suppresses transitions. (inset, bottom-right) The observed rate of microtubule jumps appears to decrease exponentially with the number of cross-linkers N. Dots show simulation estimates of the rate, whereas the line shows a least square exponential fit. In the examples, $\ell = 40$, and $N = 12$ for the time trace.

The jumping behavior causes effective Brownian motion of the microtubule with diffusion constant $D \approx \delta^2 r$ (Sec. S.III of the Supplemental Material [45]). We can estimate the effective friction coefficient of the cross-linked microtubule ζ using the Einstein relation [51],

$$\zeta = \frac{k_B T}{D} = \frac{k_B T}{\delta^2 r}. \tag{1}$$

Hence, we can focus our attention on the jump rate r, which indirectly gives the friction coefficient via Eq. (1). In Sec. S.IV of the Supplemental Material [45] we show that the friction coefficient computed via Eq. (1) agrees with that as obtained by applying an external force on the top filament, provided the system is in the linear-response regime of low force and speed, where the cross-linkers have time to reequilibrate in between the filament jumps.

The bottom-right inset of Fig. 2 shows that the jump rate r decreases roughly exponentially with the number of cross-linkers in the overlap N. This indicates that the friction coefficient ζ increases exponentially with the number of cross-linkers [Eq. (1)], whereas one would naively expect it to increase linearly with N [7,20,26,37,39,40,42].

To investigate the origin of the exponential decrease of the jump rate, we calculate the free-energy landscape as a function of two order parameters involved in the filament jumps. Without loss of generality, we focus on a jump to the right. As shown in the top-left inset of Fig. 2, a jump requires the microtubule to move one lattice spacing, and all cross-linkers need to make one net hop. The former change is captured by the microtubule position x changing from 0 to δ, and the latter change is described by the number of right-pulling cross-linkers N_R changing from 0 to N. To find the free energy as a function of the order parameters x and N_R, we first calculate the potential energy of the system,

$$\begin{aligned} U(x, N_R) &= \frac{1}{2} k x^2 (N - N_R) + \frac{1}{2} k (\delta - x)^2 N_R \\ &= \frac{1}{2} k \delta^2 N \left[\left(\frac{x}{\delta} - \frac{N_R}{N} \right)^2 + \frac{N_R}{N} \left(1 - \frac{N_R}{N} \right) \right]. \end{aligned} \tag{2}$$

All potential energy is stored in the springs, and there are N_R right-pulling linkers with stretch $\delta - x$ and $N - N_R$ left-pulling linkers with stretch x. When the values of the order parameters x and N_R are set, all microstates have the same potential energy. Hence, we can make use of Boltzmann's formula $S = k_B \log \Omega$ to calculate the entropy of the system, where $\Omega(x, N_R)$ represents the number of microstates due to different permutations of the cross-linkers in the overlap. Furthermore, the number of different permutations of the L and R linkers is independent of the position x, meaning that $\Omega(x, N_R) = \Omega(N_R)$. The Helmholtz free energy is thus

$$\begin{aligned} \mathcal{F}(x, N_R) &= U(x, N_R) - TS(x, N_R) \\ &= U(x, N_R) - k_B T \log \Omega(N_R). \end{aligned} \tag{3}$$

Surprisingly, it is possible to obtain a closed form expression for $\Omega(N_R)$ (Sec. S.V of the Supplemental Material [45]),

$$\Omega(N_R) = \binom{\ell - N_R}{N - N_R} \binom{\ell - N + N_R}{N_R}. \tag{4}$$

Intuitively, the first binomial factor represents the number of ways $N - N_R$ L linkers can be placed in an overlap with ℓ sites, when N_R of those sites are excluded by R linkers. The second factor is simply the symmetric counterpart to the first one, and counts permutations of the R linkers. With Eq. (2) and Eq. (4), we have arrived at an *exact* solution for the free-energy Eq. (3) (Sec. S.VI of the Supplemental Material [45]). Figure 3 clearly shows that a free-energy barrier exists between two minima located at $(x = 0, N_R = 0)$ and $(x = \delta, N_R = N)$, where the cross-linkers are relaxed.

As can be seen in Eq. (2), the lowest free-energy path that connects the two minima obeys $x/\delta = N_R/N$, which corresponds to the diagonal of Fig. 3. As shown in

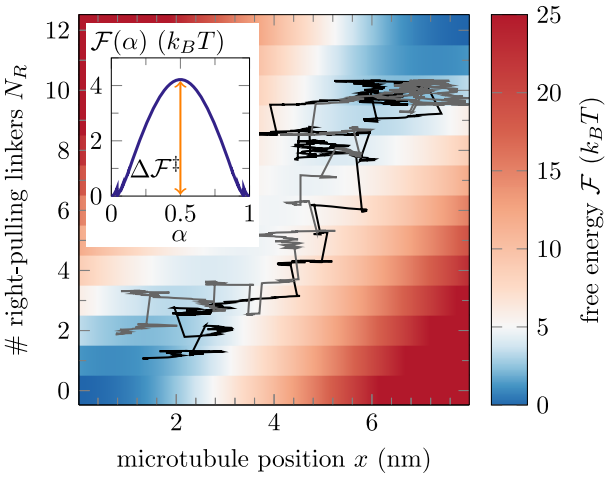

FIG. 3. Helmholtz free-energy as a function of the position x and the number of right-pulling cross-linkers N_R. Free-energy minima exist at the bottom-left and top-right corners, where the two filaments are in register and the cross-linkers are fully relaxed. These minima are separated by a free-energy barrier, where the cross-linkers are stretched (see Fig. 2). A transition over the barrier is observed as a jump of the microtubule, and two transition paths are shown for illustration. N_R is a discrete parameter, and a weak sinusoidal y offset was added to the paths to visualize their course. In this example, we use $N = 12$ and $\ell = 40$. (inset) The free-energy profile as a function of the reaction coordinate α. The height of the barrier is the difference between the Helmholtz free-energies at $\alpha = 0$ and $\alpha = 1/2$. Discontinuities occur due to the discrete nature of N_R in the definition of α.

Figs. S.11 and S.12 of the Supplemental Material [45], transition paths typically follow this diagonal, and the transition state ensemble as defined by Hummer [52] is perpendicular to it (Sec. S.VII of the Supplemental Material [45]). Therefore, the reaction coordinate is

$$\alpha = \frac{1}{2}\left(\frac{x}{\delta} + \frac{N_R}{N}\right), \tag{5}$$

which shows that the filament jumps involve a coupling between filament movement and cross-linker hops. The inset of Fig. 3 plots the free energy marginalized to α, revealing the effective barrier that the microtubule has to overcome every time it makes a $\delta = 8$ nm move.

According to Eq. (1), the friction coefficient is determined by the microtubule jump rate r, which depends on the free-energy barrier height $\Delta\mathcal{F}^{\ddagger}$ via [53]

$$r(N, \ell) = r_0(N, \ell) \exp\left[-\beta \Delta\mathcal{F}^{\ddagger}(N, \ell)\right]. \tag{6}$$

The prefactor r_0 depends on the intrinsic drag coefficients of the top filament and cross-linkers, and, at least in principle, also on the number of cross-linkers N and the number of sites in the overlap ℓ. Yet, we find that the dependence on N and ℓ is very weak, indicating that α accurately captures the reaction coordinate (Sec. S.VIII of the Supplemental Material [45]).

Our expression for the free energy, via Eqs. (2)–(4), is exact, but how it is shaped by N and ℓ remains obscure due to the discrete binomial coefficients. Therefore, we create a continuous approximation of the entropic term [54] (Sec. S.IX of the Supplemental Material [45]). We find the following simplified analytical expression for the barrier height,

$$\beta \Delta\mathcal{F}^{\ddagger} \approx A + BN \exp\left(\frac{1}{4B}\frac{N}{\ell}\right). \tag{7}$$

Here,

$$A = \frac{1}{2}\log\left(1 + \frac{3k\delta^2}{4k_BT}\right), \qquad B = \frac{k\delta^2}{8k_BT} - \log(2), \tag{8}$$

where B is positive since k is large relative to k_BT/δ^2. Figure 4 shows that this approximation is in excellent agreement with the exact result of Eqs. (2)–(4).

Since the parameter A has no N or ℓ dependence, we ignore it and absorb it in the kinetic prefactor r_0 in Eq. (6). Equation (7) then shows that when the cross-linker density N/ℓ is low, the barrier height is proportional to the number of cross-linkers N. The contribution of each linker B has an energetic and an entropic component, which can be understood intuitively by noting that at the top of the barrier, on average, $N_R = N_L = N/2$ and each linker is stretched by a distance $\delta/2$: the average potential energy per linker is then $k\delta^2/8$ (see also Fig. S.8 of the Supplemental Material [45]),

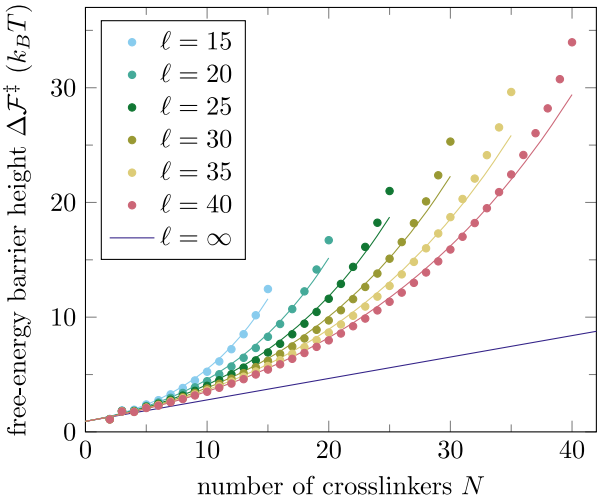

FIG. 4. The free-energy barrier height $\Delta\mathcal{F}^{\ddagger}$ increases exponentially with the number of cross-linkers N. The exact values [given by Eqs. (2), (4)], plotted as points, are approximated well by the continuous exponential curves as given by Eq. (7). Notice that the number of cross-linkers cannot exceed the number of sites on the microtubule, $N \leq \ell$. Furthermore, we plot the approximated barrier height for an infinitely long mobile microtubule, which demonstrates that the barrier height increases linearly with N when the cross-linker density N/ℓ is low. Using Eqs. (1) and (6), we predict that the friction coefficient ζ increases exponentially with N at low cross-linker densities and superexponentially with N at high densities.

while the entropy per cross-linker is log(2). At higher cross-linker densities, however, the cross-linkers increasingly block each other's hops, and the barrier scales exponentially with the cross-linker density N/ℓ.

Combining Eqs. (6), (7) and (1) shows that the friction coefficient increases exponentially with N at low cross-linker density N/ℓ but superexponentially at higher densities:

$$\zeta \propto \exp\left[BN \exp\left(\frac{1}{4B}\frac{N}{\ell}\right)\right]. \tag{9}$$

Hence, the crossover to superexponential scaling occurs when $N/\ell \approx 4B$, which means that the critical overlap length l^* at which this scaling sets in increases linearly with N. Yet, because ζ depends not only on N/ℓ but also on N separately, an overlap that is compressed at a high and constant N may effectively stall before the superexponential regime is reached, simply because the friction becomes prohibitive. For the parameter values of Table S.1 of the Supplemental Material [45] and a force of 10 pN [55] this occurs when $N \approx 20$, corresponding to $l^* \approx 200$ nm (Sec. S.X of the Supplemental Material [45]). We emphasize however that ζ depends hypersensitively on the cross-linker stiffness k and the lattice spacing δ [Eqs. (8)–(9)]; reducing k by 10 percent increases l^* threefold. Hence, different linkers, such as the actin-binder anillin [19], or even other members

from the same Ase1/PRC1 family, are expected to have markedly different l^*.

In conclusion, our work has revealed how passive cross-linkers cause friction between filaments. If the cross-linkers were to bind to a continuum of binding sites, then the friction coefficient would scale linearly with the number of cross-linkers, as predicted by previous models [7,20,26,37,39–42]. However, cytoskeletal filaments such as microtubules consist of discrete units, yielding discrete binding sites for the cross-linkers. Moreover, cross-linkers such as Ase1/PRC1 are stiff on the scale of the spacing between the binding sites ($k\delta^2 > k_BT$). These two factors together mean that the filaments can only move if the cross-linkers reorganize collectively. This creates a free-energy barrier for filament movement which scales exponentially with the density of cross-linkers [Eq. (7)]. Since the friction between the filaments depends exponentially on the height of the free-energy barrier, the friction depends superexponentially on the density of cross-linkers. In Sec. S.XI of the Supplemental Material [45] we show that cooperative interactions between cross-linkers [5,56] do not alter the fundamental mechanism for friction generation, and the fricton coefficient continues to scale superlinearly with N. While we have studied here a single-protofilament model, we expect that multiprotofilaments exhibit the same scaling, because multiple protofilaments do not alter the basic mechanism that underlies the scaling: filaments jumping between positions where the cross-linker stretching energy is minimized.

The highly nonlinear dependence of the friction coefficient ζ on the number of cross-linkers N and the overlap length ℓ has implications in biology, both for the formation of the mitotic spindle [1–15] and the cytokinetic ring [16–19]. Equation (8) shows that the key parameters that control the scaling of ζ with N and ℓ are the lattice spacing δ and the protein stiffness k. To understand the contraction speed of the cytokinetic ring, it will be of interest to estimate k for cross-linkers like anillin [19] since it will determine how rapidly the friction rises when the ring contracts. In the mitotic spindle microtubules are pushed apart by plus-end directed motor proteins [6,11,13,14,57–60]. Our results indicate that the friction generated by proteins from the Ase1/PRC1 family is highly sensitive to the cross-linker density. As a result, a shrinking overlap region undergoes a sudden increase in the friction coefficient, which will effectively stall the microtubules. Hence, steric hindrance imposes stable overlaps not only by opposing motor stepping [13] but also by dramatically increasing the friction. The overlap length can be fine-tuned by controlling the number of cross-linkers contained in the overlap, for example, by reducing the binding affinity of PRC1 to microtubules through phosphorylation [44].

Our work yields a number of predictions that can be tested experimentally. First, it predicts that cross-linked filaments move via discrete jumps, which can be tested via *in vitro* gliding assays using microtubules coated with quantum dots, allowing for nanometer precision [61]. Optical tweezers with sub-pN and nanometer resolution could be used to directly measure the free-energy profile [62]. But the most interesting test would be to measure the friction coefficient as a function of N and ℓ, either via the diffusion constant and the Einstein relation [Eq. (1)] [21], or via an applied load using a stiff optical trap (Sec. S.IV of the Supplemental Material [45]). Different filament-cross-linker systems, with different protein stiffness k and lattice spacing δ, are now accessible *in vitro* [19,21], which should make it possible to test the predicted scaling of Eq. (9).

The authors thank Z. Lansky, M. Braun, and S. Diez for the fruitful collaboration, and B. M. Mulder for assessing the manuscript. This work was supported by European Research Council (ERC) Synergy Grant No. 609822, is part of the research programme of the Netherlands Organisation for Scientific Research (NWO), and performed at the research institute AMOLF.

*tenwolde@amolf.nl

[1] A. Yamashita, M. Sato, A. Fujita, M. Yamamoto, and T. Toda, Mol. Biol. Cell **16**, 1378 (2005).
[2] I. Loïodice, J. Staub, T. G. Setty, N.-P. T. Nguyen, A. Paoletti, and P. T. Tran, Mol. Biol. Cell **16**, 1756 (2005).
[3] M. E. Janson, R. Loughlin, I. Loïodice, C. Fu, D. Brunner, F. J. Nédélec, and P. T. Tran, Cell **128**, 357 (2007).
[4] T. Courtheoux, G. Gay, Y. Gachet, and S. Tournier, J. Cell Biol. **187**, 399 (2009).
[5] R. Subramanian, E. M. Wilson-Kubalek, C. P. Arthur, M. J. Bick, E. A. Campbell, S. A. Darst, R. A. Milligan, and T. M. Kapoor, Cell **142**, 433 (2010).
[6] P. Bieling, I. A. Telley, and T. Surrey, Cell **142**, 420 (2010).
[7] C. Hentrich and T. Surrey, J. Cell Biol. **189**, 465 (2010).
[8] M. Braun, Z. Lansky, G. Fink, F. Ruhnow, S. Diez, and M. E. Janson, Nat. Cell Biol. **13**, 1259 (2011).
[9] R. Subramanian, S.-C. Ti, L. Tan, S. A. Darst, and T. M. Kapoor, Cell **154**, 377 (2013).
[10] D. Johann, D. Goswami, and K. Kruse, Phys. Rev. E **93**, 062415 (2016).
[11] R. Blackwell, C. Edelmaier, O. Sweezy-Schindler, A. Lamson, Z. R. Gergely, E. O'Toole, A. Crapo, L. E. Hough, J. R. McIntosh, M. A. Glaser, and M. D. Betterton, Sci. Adv. **3**, e1601603 (2017).
[12] S. A. Rincon, A. Lamson, R. Blackwell, V. Syrovatkina, V. Fraisier, A. Paoletti, M. D. Betterton, and P. T. Tran, Nat. Commun. **8**, 15286 (2017).
[13] S. Wijeratne and R. Subramanian, eLife **7**, e32595 (2018).
[14] J. Hannabuss, M. Lera-Ramirez, N. I. Cade, F. J. Fourniol, F. Nédélec, and T. Surrey, Curr. Biol. **29**, 2120 (2019).
[15] A. R. Lamson, C. J. Edelmaier, M. A. Glaser, and M. D. Betterton, Biophys. J. **116**, 1719 (2019).
[16] Z. Xue and A. M. Sokac, J. Cell Biol. **215**, 335 (2016).
[17] R. Neujahr, C. Heizer, and G. Gerisch, J. Cell Sci. **110**, 123 (1997), https://jcs.biologists.org/content/110/2/123.
[18] X. Ma, M. Kovács, M. A. Conti, A. Wang, Y. Zhang, J. R. Sellers, and R. S. Adelstein, Proc. Natl. Acad. Sci. U.S.A. **109**, 4509 (2012).

[19] O. Kučera, D. Janda, V. Siahaan, S. H. Dijkstra, E. Pilátová, E. Zatecka, S. Diez, M. Braun, and Z. Lansky, bioRxiv, https://doi.org/10.1101/2020.01.22.915256 (2020).

[20] S. Walcott and S. X. Sun, Phys. Rev. E **82**, 050901(R) (2010).

[21] Z. Lansky, M. Braun, A. Lüdecke, M. Schlierf, P. R. ten Wolde, M. E. Janson, and S. Diez, Cell **160**, 1159 (2015).

[22] A. Ward, F. Hilitski, W. Schwenger, D. Welch, A. W. C. Lau, V. Vitelli, L. Mahadevan, and Z. Dogic, Nat. Mater. **14**, 583 (2015).

[23] S. Mukhina, Y.-L. Wang, and M. Murata-Hori, Dev. Cell **13**, 554 (2007).

[24] E. M. Reichl, Y. Ren, M. K. Morphew, M. Delannoy, J. C. Effler, K. D. Girard, S. Divi, P. A. Iglesias, S. C. Kuo, and D. N. Robinson, Curr. Biol. **18**, 471 (2008).

[25] T. D. Pollard, Curr. Opin. Cell Biol. **22**, 50 (2010).

[26] S. Forth, K.-C. Hsia, Y. Shimamoto, and T. M. Kapoor, Cell **157**, 420 (2014).

[27] Y. Ezber, V. Belyy, S. Can, and A. Yildiz, Nat. Phys. **16**, 312 (2020).

[28] A. Vanossi, N. Manini, M. Urbakh, S. Zapperi, and E. Tosatti, Rev. Mod. Phys. **85**, 529 (2013).

[29] V. Bormuth, V. Varga, J. Howard, and E. Schäffer, Science **325**, 870 (2009).

[30] H. Suda, Langmuir **17**, 6045 (2001).

[31] A. F. Huxley, Prog. Biophys. Biophys. Chem. **7**, 255 (1957).

[32] C. S. Peskin, *Partial Differential Equations in Biology* (Courant Institute of Mathematical Sciences, New York University, 1976).

[33] H. M. Lacker, Cross-bridge dynamics in skeletal muscle: Mathematical methods for determining the reaction rate and force-extension curves of cross-bridges from the macroscopic behavior of muscle, Ph.D. thesis, New York University, New York, 1977.

[34] H. M. Lacker and C. S. Peskin, *Some Mathematical Questions in Biology—Muscle Physiology* (American Mathematical Society (AMS), Providence, Rhode Island, 1986), pp. 121–153.

[35] T. a. J. Duke, Proc. Natl. Acad. Sci. U.S.A. **96**, 2770 (1999).

[36] M. Srinivasan and S. Walcott, Phys. Rev. E **80**, 046124 (2009).

[37] S. Walcott and S. X. Sun, Proc. Natl. Acad. Sci. U.S.A. **107**, 7757 (2010).

[38] S. Forth and T. M. Kapoor, J. Cell Biol. **216**, 1525 (2017).

[39] K. Tawada and K. Sekimoto, J. Theor. Biol. **150**, 193 (1991).

[40] S. Leibler and D. A. Huse, J. Cell Biol. **121**, 1357 (1993).

[41] M. Lera-Ramirez and F. J. Nédélec, Cytoskeleton (Hoboken) **76**, 600 (2019).

[42] B. Harland, S. Walcott, and S. X. Sun, Phys. Biol. **8**, 015011 (2011).

[43] L. A. Amos and A. Klug, J. Cell Sci. **14**, 523 (1974), https://jcs.biologists.org/content/14/3/523.

[44] E. H. Kellogg, S. Howes, S.-C. Ti, E. Ramírez-Aportela, T. M. Kapoor, P. Chacón, and E. Nogales, Proc. Natl. Acad. Sci. U.S.A. **113**, 9430 (2016).

[45] See Supplemental Material at http://link.aps.org/supplemental/10.1103/PhysRevLett.125.078101 for details of derivations and computational algorithms.

[46] S. Jeney, E. H. K. Stelzer, H. Grubmüller, and E.-L. Florin, Chem. Phys. Chem. **5**, 1150 (2004).

[47] M. Schlierf and M. Rief, J. Mol. Biol. **354**, 497 (2005).

[48] H. Ahmadzadeh, D. H. Smith, and V. B. Shenoy, Biophys. J. **106**, 1123 (2014).

[49] A. J. Hunt, F. Gittes, and J. Howard, Biophys. J. **67**, 766 (1994).

[50] A. Prados, J. J. Brey, and B. Sánchez-Rey, J. Stat. Phys. **89**, 709 (1997).

[51] A. Einstein, Ann. Phys. (Berlin) **322**, 549 (1905).

[52] G. Hummer, J. Chem. Phys. **120**, 516 (2004).

[53] S. Arrhenius, Z. Phys. Chem. **4U**, 226 (1889).

[54] P. Milewski, Derivation of Gaussian Distribution from Binomial (2007), accessed online on 2018-11-22.

[55] M. C. Uçar and R. Lipowsky, Nano Lett. **20**, 669 (2020).

[56] L. C. Kapitein, M. E. Janson, S. M. J. L. van den Wildenberg, C. C. Hoogenraad, C. F. Schmidt, and E. J. G. Peterman, Curr. Biol. **18**, 1713 (2008).

[57] L. C. Kapitein, E. J. G. Peterman, B. H. Kwok, J. H. Kim, T. M. Kapoor, and C. F. Schmidt, Nature (London) **435**, 114 (2005).

[58] C. Fu, J. J. Ward, I. Loiodice, G. Velve-Casquillas, F. J. Nedelec, and P. T. Tran, Dev. Cell **17**, 257 (2009).

[59] Y. Shimamoto, S. Forth, and T. M. Kapoor, Dev. Cell **34**, 669 (2015).

[60] C. J. Edelmaier, A. R. Lamson, Z. R. Gergely, S. Ansari, R. Blackwell, J. R. McIntosh, M. A. Glaser, and M. D. Betterton, eLife, **9** e48787 (2020).

[61] C. Leduc, F. Ruhnow, J. Howard, and S. Diez, Proc. Natl. Acad. Sci. U.S.A. **104**, 10847 (2007).

[62] K. C. Neuman and A. Nagy, Nat. Methods **5**, 491 (2008).